Journal of the Ceramic Society of Japan 117 [4] 475-481 2009 Special Article
The 62th CerSJ Awards for Advancements in Ceramic Science and Technology: Review

Interface structure and polarity of GaN/ZnO heterostructure

Takeshi OHGAKI†

Sensor Materials Center, National Institute for Materials Science, 1−1, Namiki, Tsukuba, Ibaraki 305−0044

Gallium nitride (GaN) films were grown with and without lattice-matched (In,Ga)N buffer layers on the c(+) and c(–) faces of ZnO single-crystal substrates using molecular beam epitaxy, and their interface structures, including the relationship between the crystallinity of the GaN film and the polarity of the ZnO substrate, were investigated. Growth at a high temperature (e.g., 800°C) was made possible by using an (In,Ga)N buffer layer, which improved the crystallinity of the GaN films compared with that of GaN films grown directly on a ZnO substrate. Ion scattering, i.e., coaxial impact-collision ion scattering spectroscopy, and electron beam channeling, i.e., convergent beam electron diffraction, profiles revealed that the GaN films grown on c(+)- and c(–)-ZnO substrates with an (In,Ga)N buffer layer had a (0001) surface (i.e., c(+) polarity). That is, polarity inversion occurs when GaN film is grown with an (In,Ga)N buffer layer on a c(–)-ZnO substrate.

Key-words : Wurtzite-type lattice, Gallium nitride, Zinc oxide, Molecular beam epitaxy, Interface structure, Polarity, Buffer layer

[Received October 23, 2008]

1. Introduction

Light emitting diodes (LEDs) made of gallium nitride (GaN) related alloys (III–V nitrides) are now commercially available due to improvements in the growth techniques used for new process and efficient doping.[1)–4)] Although lattice-matched substrates are essentially suitable for epitaxial growth of high-quality single-crystal film, most commercial GaN-based diodes are prepared on sapphire (α-Al_2O_3) or silicon-carbide (SiC) substrates likely due their lower cost. Further improvement in the performance of GaN-related devices requires the use of a substrate more suitable for growing high-quality GaN films. Several trials of growing highly crystalline GaN films have been carried out using various substrates other than α-Al_2O_3 and SiC.[5)–7)]

In the search for useful substrates for III–V nitride growth, zinc oxide (ZnO) was identified as a promising candidate as a lattice-matched substrate because GaN and ZnO have the same lattice symmetry, i.e., wurtzite, and their lattice constants are nearly the same. The lattice mismatch between GaN and ZnO on the c-plane is –1.9%, which is much less than that between GaN and α-Al_2O_3 on the c-plane (16%). Moreover, ZnO has novel emission properties:[8),9)] transparency to visible light[10),11)] and high electrical conductivity after doping.[12),13)] The functions of GaN/ZnO heterostructures are also attracting attention, and these heterostructures have been studied theoretically[14),15)] and experimentally[16),17)] with the aim of using them to fabricate optoelectronic devices composed of GaN/ZnO heterojunctions. There have already been reports on blue-light emission in LED devices composed of n-type ZnO and p-type GaN.[18)–20)] Improving the performance of such devices and developing new devices made from GaN/ZnO heterostructures require an understanding of the interfaciel structure at the GaN/ZnO boundary. Unfortunately, there have been few reports on the interfaciel structure of GaN/ZnO heterostructures.[21),22)]

The crystalline polarity of GaN and ZnO is another important issue in the development of optoelectronic devices fabricated using GaN and ZnO. Since a wurtzite-type structure lacks inversion symmetry, GaN and ZnO are permanently polarized along the *c*-axis of their lattice and exhibit pyroelectricity and piezoelectricity. Such polarization in III–V nitride semiconductors affects the properties of LEDs[23)] and transistors.[24)] The crystalline polarity of ZnO strongly affects its chemical[25)–27)] and physical[28)] properties, which motivated us to investigate the polarity relationship at the GaN/ZnO interface.

The GaN films grown on ZnO substrates were prepared using molecular beam epitaxy (MBE) and investigated their interfaciel structures in terms of the crystalline polarity relationship between the GaN film and ZnO substrate. Also investigated was the effect of using a lattice-matched (In,Ga)N buffer layer at the GaN/ZnO interface on the crystallinity of the GaN film.

2. Experimental procedure

ZnO single crystals grown using the hydrothermal method were used as the substrate, and two crystalline orientations of the substrate were examined: (0001) Zn-face and $(000\bar{1})$ O-face of ZnO. Hereafter, "GaN/c(+)-ZnO" and "GaN/c(–)-ZnO" represent GaN film deposited on the (0001) and $(000\bar{1})$ faces, respectively, of ZnO. The orientations were determined using chemical etching with dilute hydrochloric-acid solution.[29)] Prior to film growth, the substrates were thermally treated to obtain atomically flat surfaces with neither mechanical damage nor scratches caused by imperfect chemical-mechanical polishing.[26)] During heat treatment, ZnO single crystals were fully covered by single-crystalline Y-doped ZrO_2 plates to prevent obvious evaporation of the Zn and contamination from the environment.

To examine the effect of using a lattice-matched buffer layer at the GaN/ZnO interface, two types of samples were prepared: GaN/ZnO structures prepared using direct deposition of a GaN layer on a ZnO substrate and GaN/InGaN/ZnO structures in which a lattice-matched (In,Ga)N buffer layer was inserted at the GaN/ZnO interface. Since the lattice parameters of $(In_{1-x}Ga_x)N$ (x = 0.2) are close to those of ZnO, an $(In_{0.2}Ga_{0.8})N$ layer was used as the lattice-matched buffer layer. Both types of samples were prepared using MBE. A conventional Knudsen cell with a tantalum

† Corresponding author: T. Ohgaki; E-mail: OGAKI.Takeshi@nims.go.jp

crucible was used for evaporating the Ga (99.999999%) and In (99.9999%). The film surface was irradiated with a nitrogen radical beam to nitridate the evaporated Ga and In during deposition. Nitrogen radicals were generated with an RF (13.56 MHz) discharge cell. Pure nitrogen gas (99.9999%) was continuously introduced into the discharge cell, and the total pressure in the growth chamber was kept at 3.5–4.0 × 10^5 Torr. Film growth was initiated by exposing the ZnO surface simultaneously to incident Ga (Ga and In) and N flux; therefore, no pre-deposition treatment, such as nitridation and metallization of the substrate surface, was used. The GaN/ZnO structures were grown at 730°C. For the GaN/InGaN/ZnO structures, a 30-nm-thick $(In_{0.2}Ga_{0.8})N$ buffer layer was first grown at 550°C on a ZnO surface, and then a GaN layer was grown at 800°C on the (In,Ga)N layer. To prevent phase separation of the (In,Ga)N layer at this high temperature, Ga and N flux was supplied to the film surface when the substrate temperature was increased from 550 to 800°C. The total thickness of the GaN films with and without a buffer layer was set to ~500 nm.

The lattice orientation and crystallinity of the GaN films were determined by X-ray diffraction (XRD) (θ–2θ mode, ω-scan mode, pole figure, and reciprocal space mapping) and by selected area electron diffraction using transmission electron microscopy (TEM). The interdiffusion of Zn, Ga, In, O, and N during film growth was measured using an energy-dispersive X-ray spectroscope attached to the TEM apparatus. The polarities of the films were analyzed using coaxial impact-collision ion scattering spectroscopy (CAICISS).[30] The incident He^+ ion beam had an energy of 2 keV, and the focused beam spot size was less than 3 mm in diameter. The kinetic energy of the back-scattered ions was analyzed with a time-of-flight detector. The atomic arrangement in the topmost surface was determined by fitting the observed CAICISS spectra to that of ZnO single crystals. The convergent beam electron diffraction (CBED) technique, which is considered an appropriate way to determine the crystalline polarity of GaN crystals,[31] was used to investigate the polarity of the GaN films.

3. Results and discussion

3.1 Effects of substrate polarity and buffer layer on film structure

The GaN/c(+)-ZnO and GaN/c(–)-ZnO were highly *c*-axis oriented regardless of the presence of a lattice-matched (In,Ga)N buffer layer. The (0002) and (0004) diffraction peaks of GaN were observed as well as ZnO diffraction peaks in the XRD profiles for θ–2θ mode. Only six sharp spots corresponding to GaN $(10\bar{1}1)$ diffraction were observed for the same in-plane orientation of ZnO $(10\bar{1}1)$ diffraction in the X-ray pole figure patterns. This indicates that the in-plane orientation of the GaN/c(+)-ZnO and GaN/c(–)-ZnO was locked and that no rotational domain formed in the films.

The microstructure of the GaN films directly deposited on ZnO substrates were remarkably dependent on the substrate's polarity. **Figure 1** shows cross-sectional TEM images of the GaN/ZnO structures. The GaN/c(+)-ZnO (Fig. 1(a)) had a rough surface and was composed of columnar grains 50–200 nm in radius. The GaN/c(–)-ZnO (Fig. 1(b)) had a smooth surface, and there were many threading dislocations parallel to the growth direction. It should be noted that the latter film peeled off the substrate during preparation of the sample for TEM observation. The threading dislocation density evident in the image shown in Fig. 1(a) was less than in that shown in (b), and there are fringe patterns due to non-uniform internal stress. These results indicate that the stress due to lattice mismatch between GaN and ZnO relaxed depending on the polarity of the ZnO substrate. This substrate polarity dependence has also been found in InN/ZnO structures,[32] which is why the CAICISS spectra for the GaN layers in the GaN/InGaN/ZnO structures was examined in this study.

Figure 2 shows X-ray reciprocal space maps of the $(11\bar{2}4)$ diffraction for the GaN films directly deposited on ZnO substrates. Comparison of the one for the GaN/c(+)-ZnO structure (Fig. 2(a)) with that for the GaN/c(–)-ZnO structure (Fig. 2(b)) reveals two significant differences: the spot size of the ZnO $(11\bar{2}4)$ diffraction and the shape of the GaN $(11\bar{2}4)$ diffraction spot. The diffraction pattern for the GaN/c(+)-ZnO structure shows a broadening of the ZnO $(11\bar{2}4)$ diffraction spot. As mentioned above, a fringe pattern attributed to non-uniform internal stress at the GaN/ZnO interface region was found in the TEM image of the GaN/c(+)-ZnO structure. This broadening is well explained by non-uniform strain in both the ZnO and GaN lattices in the interface region. In contrast, obvious broadening of the ZnO $(11\bar{2}4)$ diffraction spot is not found in the profile for the GaN/c(–)-ZnO structure. These results imply that the relaxation of the lattice mismatch at the GaN/ZnO interface depends on the polarity of the ZnO substrate. Moreover, the shape of the GaN $(11\bar{2}4)$ diffraction spot depends on the polarity of the substrate. As shown in Fig. 2(a), the GaN $(11\bar{2}4)$ diffraction spot for the GaN/c(+)-ZnO structure was oval, and its major axis direction is explained by assuming a slight tilt of the GaN lattice axis from the ZnO lattice axis. In other words, the broadening of the

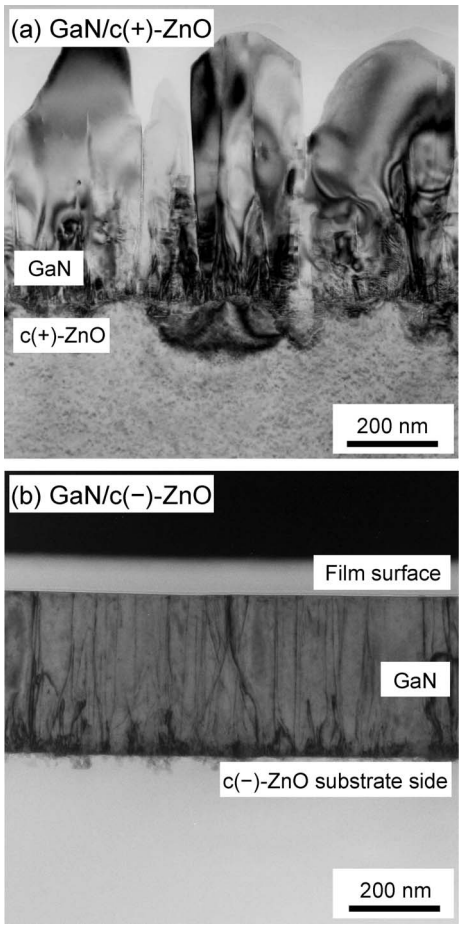

Fig. 1. TEM images of GaN films without (In,Ga)N buffer layer grown on (a) c(+)-ZnO and (b) c(–)-ZnO substrates. GaN film grown on c(–)-ZnO substrate peeled off during sample preparation for TEM observation.

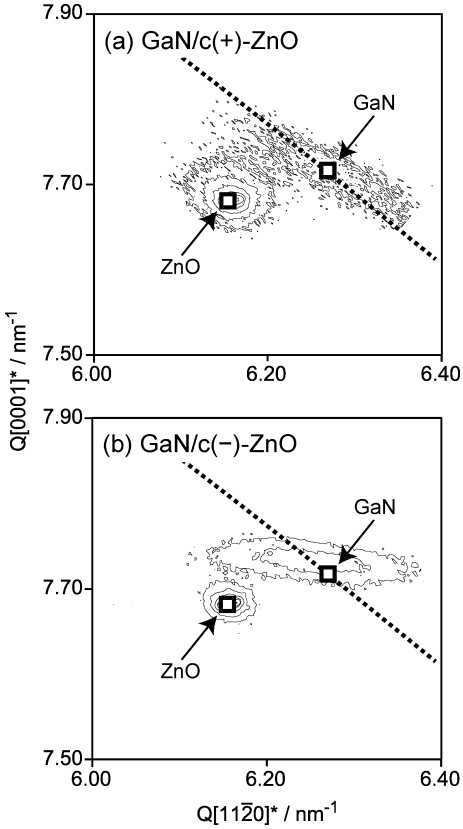

Fig. 2. (11$\bar{2}$4) X-ray reciprocal space maps of GaN films without (In,Ga)N buffer layer grown on (a) c(+)-ZnO and (b) c(–)-ZnO substrates. Open squares indicate expected diffraction positions of ZnO and GaN single crystals. Dotted lines indicate expected diffraction position of polycrystalline GaN.

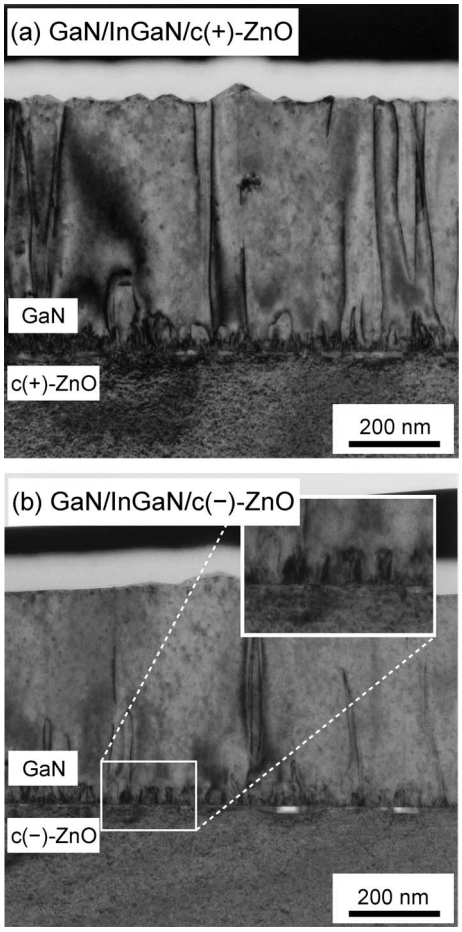

Fig. 3. TEM images of GaN films deposited on (a) c(+)-ZnO and (b) c(–)-ZnO substrates covered with (In,Ga)N buffer layer. Insert shows magnified image of area marked in (b).

GaN (11$\bar{2}$4) diffraction spot for the GaN/c(+)-ZnO structure lie on the diffraction line of the polycrystalline GaN, each grain of which has the same lattice parameters, while the grain orientations are slightly disordered. Therefore, the lattice mismatch at the GaN/c(+)-ZnO interface likely caused non-uniform strain in the ZnO layer and a slight tilt of the GaN lattice axis from the ZnO lattice axis. Although the GaN (11$\bar{2}$4) diffraction spot for the GaN/c(–)-ZnO structure was also oval, its major axis direction was different: its GaN (11$\bar{2}$4) diffraction spot extended along the [11$\bar{2}$0]* axis. This means that the in-plane lattice parameter of GaN on the c(–)-ZnO substrate was elongated due to restriction by the ZnO lattice in the interfaciel region and that the values of the lattice parameters approached those for bulk GaN as the film thickness increased. This is consistent with the TEM image shown in Fig. 1(b), which shows that threading dislocations formed and reduced the stress caused by lattice mismatch. These results clearly show that the manner in which internal stress due to lattice mismatch is relaxed depends on the polarity of the ZnO substrate. The results of the microstructure observation and crystallographic analysis are consistent for the GaN/ZnO structures without a buffer layer.

The microstructures of the GaN/InGaN/ZnO structures are shown in **Fig. 3**. The GaN films with a (In,Ga)N buffer layer had a relatively smooth surface regardless of the substrate's polarity, and the columnar grains found in the GaN/c(+)-ZnO structure (Fig. 1(a)) were not observed even in the GaN/InGaN/c(+)-ZnO structure using c(+)-ZnO as the substrate. These film structures with a (In,Ga)N layer were similar to GaN film directly grown on a c(–)-ZnO substrate. Moreover, the threading dislocation density in the GaN/InGaN/ZnO structures was clearly less than that in the GaN/c(–)-ZnO structure shown in Fig. 1(b). In addition, these images show that the dislocations disappeared as the film thickened, although high dislocation density was found in the GaN layer in the interfaciel region, as shown in the inset of Fig. 3(b). Thus, it is clear that the insertion of an (In,Ga)N buffer layer at the interface improved the crystallinity of the GaN layers, and the high dislocation density in the interface region may contribute to the relaxation of stress in this region.

As the TEM images for the GaN/InGaN/ZnO structures were similar to that for the GaN/c(–)-ZnO structure, the X-ray diffraction patterns for the GaN/InGaN/ZnO structures were similar to that for the GaN/c(–)-ZnO structure, regardless of the substrate's polarity. As shown in **Fig. 4**, the (11$\bar{2}$4) diffraction for the GaN layer in the GaN/InGaN/c(–)-ZnO structure was oval and expanded nearly parallel to the [11$\bar{2}$0]* axis. This implies that the values of the a- and b-parameters of the GaN lattice expanded from restriction by the ZnO substrate similar to GaN/c(–)-ZnO. The only difference between the GaN/c(–)-ZnO and GaN/InGaN/c(–)-ZnO structures was the size of the (11$\bar{2}$4) spot in the GaN layer. The GaN/InGaN/c(–)-ZnO structure had a smaller spot. The spot size roughly corresponded to the dislocation density in the GaN layer. The GaN/InGaN/c(–)-ZnO structure showed a smaller (11$\bar{2}$4) spot of the GaN layer and less dislocation density than those of the GaN/c(–)-ZnO structure.

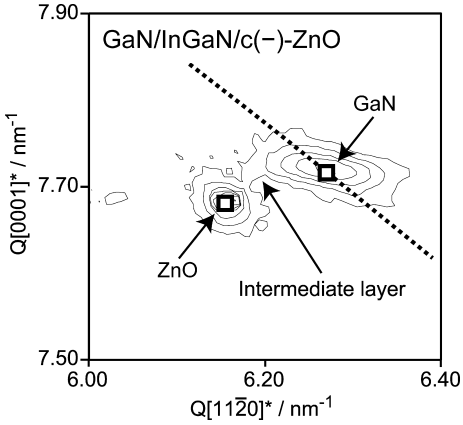

Fig. 4. (11$\bar{2}$4) X-ray reciprocal space map of GaN film with (In,Ga)N buffer layer grown on c(–)-ZnO substrate. Open squares indicate expected diffraction positions of ZnO and GaN single crystals. Dotted line indicates expected diffraction position of polycrystalline GaN.

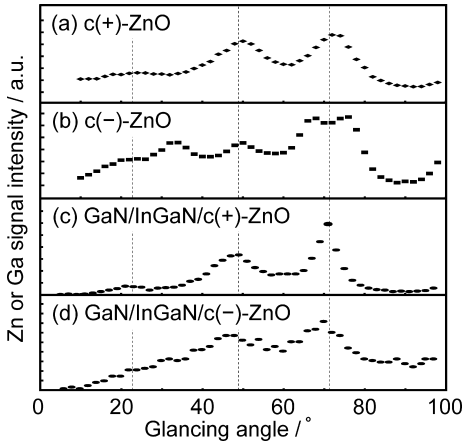

Fig. 5. Glancing angle dependency of Zn or Ga signal intensity along [11$\bar{2}$0] azimuth: (a) c(+)-ZnO single crystal, (b) c(–)-ZnO single crystal, (c) GaN film with (In,Ga)N buffer layer grown on c(+)-ZnO substrate, and (d) GaN film with (In,Ga)N buffer layer grown on c(–)-ZnO substrate.

It was also interesting that the presence of an intermediate layer between the ZnO substrate and the GaN layer was indicated in the diffraction profile, as marked by arrows in Fig. 4. This suggests that an (In,Ga)N layer between the substrate and GaN film acts as a buffer layer that gradually relaxes the lattice mismatch between GaN and ZnO. As shown in the TEM image of Fig. 3(b), the density of the dislocations in the interface region was high, and these dislocations may be the origin of the intermediate layer for which a trace was found in the X-ray diffraction profile.

It is also notable that the use of the (In,Ga)N buffer layer enabled the deposition of GaN films at a relatively high temperature, e.g., 800°C. The GaN layers were deposited directly on the ZnO substrate at $T > 730$°C, and they peeled off the substrate during and after deposition. This was the reason a relatively low temperature ($T = 730$°C) was used in depositing the GaN/ZnO structures. Insertion of the (In,Ga)N buffer layer improved the bonding strength between the GaN layer and ZnO substrate, and growing GaN at a relatively high temperature, e.g., 800°C, was possible when ZnO substrates were used with an (In,Ga)N buffer layer. The gradual relaxation of the stress due to lattice mismatch, as revealed by the XRD pattern in Fig. 4, explains the high peel-off resistance of the GaN layers in the GaN/InGaN/ZnO structures. Therefore, insertion of an (In,Ga)N buffer layer is the key to obtaining highly crystalline GaN layers on ZnO substrates.

3.2 Polarity relationship of GaN/ZnO heterostructure

The polarity of the ZnO substrate also affected the crystalline polarity of the GaN layer. **Figure 5** shows the CAICISS spectra obtained from the GaN film surfaces and those obtained from the surfaces of the ZnO substrates. It shows glancing angle dependencies of the CAICISS signal observed along the [0001] or [000$\bar{1}$] to [11$\bar{2}$0] direction. The CAICISS spectra of the GaN layers were obtained from the GaN surfaces of the GaN/InGaN/ZnO structures. The polarity of the GaN films was determined by assuming that the CAICISS spectra of the c(+) and c(–) faces of GaN show profiles similar to those of the c(+) and c(–) faces, respectively, of ZnO.[33),34)] As shown in Figs. 5(a) and (b), the CAICISS spectra obtained from the c(+)- and c(–)-ZnO surfaces were similar to previously reported ones.[35)] Since the spectral profiles for c(+)- and c(–)-ZnO differ, CAICISS is regarded as a good way to determine the crystalline polarity of wurtzite-type crystals. The CAICISS spectra of the GaN surfaces of the GaN/InGaN/c(+)-ZnO (Fig. 5(c)) and GaN/InGaN/c(–)-ZnO (Fig. 5(d)) structures were similar, and both were also similar to the spectrum obtained from the c(+)-ZnO surface (Fig. 5(a)). These results indicate that GaN films deposited by applying an (In,Ga)N buffer layer have a (0001) surface (i.e., c(+) polarity) regardless of the ZnO substrate's polarity. In other words, polarity inversion occurs when GaN film is grown with an (In,Ga)N buffer layer on a c(–)-ZnO substrate.

Although well-defined CAICISS spectra were obtained from the GaN surfaces of the GaN/InGaN/ZnO structures, the CAICISS spectra obtained from the GaN surfaces of the GaN/ZnO structures showed a poor signal/noise ratio, which was attributed to low crystallinity and/or surface roughness. A tilt of the GaN lattice from the ZnO lattice was observed, as were many threading dislocations in the GaN/ZnO structures, as shown in Figs. 1 and 2. An attempt was made to determine the polarity of the GaN films in the GaN/ZnO structures by assuming a correlation between the microstructure and GaN film polarity. Previous reports on the crystalline polarity and microstructure of MOCVD-grown GaN layers, e.g., that by Sumiya et al.,[33)] were used to classify the GaN films into two types. One type is characterized by a columnar structure, and most of the films of this type had a (000$\bar{1}$) surface (c(–) surface). The other type is characterized by single-crystal-like GaN layers with threading dislocations, and most of the films of this type had a (0001) surface (c(+) surface). The same relationship between crystalline polarity and microstructure was reported for MBE-grown GaN films.[36),37)] The two different growth modes were attributed to the crystal habit of a wurtzite-type lattice because the same relationship has been observed in ZnO film growth, and ZnO has the same crystal structure as GaN.[35),38)] The CAICISS results for the GaN/InGaN/ZnO structures are in agreement with this tendency. The GaN layers in the GaN/InGaN/ZnO structures were single-crystal-like films with threading dislocations (not a columnar structure), as shown in Fig. 3, and they had c(+) surfaces. This indicates that single-crystal-like GaN films with threading dislocations have a c(+) surface and that GaN films with columnar structures have a c(–) surface. If this is correct, GaN film grown directly on a c(+)-ZnO substrate, characterized by a columnar structure (Fig. 1(a)), has a c(–) surface, and GaN film grown directly on a c(–)-ZnO substrate, characterized by a microstructure

with threading dislocations (Fig. 1(b)), has a c(+) surface. This suggests that polarity inversion occurred in the GaN/ZnO structures without buffer layers regardless of the substrate's polarity. The polarity relationships determined above are listed in **Table 1**.

3.3 Polarity inversion mechanism

The results of the CAICISS analysis indicated that GaN layers with c(+) faces grew on a c(–)-ZnO substrate regardless of the presence of a buffer layer. This indicates that there should be a layer or slab (X-layer) causing polarity inversion, such as c(+)-GaN/X/c(–)-GaN/c(–)-ZnO or c(+)-GaN/X/c(–)-ZnO. The polarity inversion behavior was investigated in detail by observing the position dependence of CBED patterns along the growth direction of the GaN layer. **Figure 6** shows a TEM image of the GaN/InGaN/c(–)-ZnO structure and two typical CBED patterns obtained from regions A and B indicated in the image. The observed and theoretically calculated CBED patterns were compared. The simulations were carried out assuming that GaN film with a c(+) surface was grown on a substrate. The simulated and observed patterns were in good agreement, indicating that the GaN in both regions had the same polarity and thus had a c(+) surface. Although the CBED pattern was observed only along the growth direction, all CBED patterns obtained from the GaN/InGaN region showed patterns similar to those for regions A and B. This means that there was no polarity inversion in the nitride layer, such as c(+)-GaN/X/c(–)-GaN, in the samples. It is reasonable to assume that polarity inversion, such as c(+)-GaN/X/c(–)-ZnO, in the GaN/InGaN/c(–)-ZnO structure occurred at the GaN/ZnO interface. Several groups have reported that Ga_2O_3[21),39)] and/or $ZnGa_2O_4$[36)] phases are easily formed at the GaN/ZnO interface. For example, Hong et al.[21)] discussed polarity inversion such as c(–)-ZnO/Ga_2O_3/c(+)-GaN. Thus, Ga_2O_3 phase may act as an X-layer and form c(+)-GaN/X/c(–)-ZnO structures.

However, the presence of a relatively thick interfaciel layer was not found in the GaN/InGaN/c(–)-ZnO structure. **Figure 7(a)** shows a high-resolution TEM image of the c(+)-GaN/InGaN/c(–)-ZnO interface. Although polarity inversion occurred in this structure, there was no clear trace of an interfaciel phase, such as a Ga_2O_3 or Ga_2ZnO_4 layer. Figure 7(b) shows a magnified image of the interface. The spacing of the horizontal lines corresponds to half of the c-parameter value of the GaN and ZnO lattices. As shown in Fig. 7(b), discontinuity of the periodicity was found in a particular layer indicated by the arrows to the left of the TEM image, and this layer may correspond to the interface between GaN (or InGaN) and ZnO. Assuming that the relatively dark spot in this image corresponds to relatively heavy elements (Zn, Ga, and In), the observed images suggest the presence of an extrinsic layer about a quarter the thickness of the c-parameter value of ZnO. This means that the observed polarity inversion occurred due to formation of this interfaciel layer. The same polarity inversion relationship and discontinuity of the periodicity were previously found in InN/ZnO heterostructures.[40)] It

Table 1. Effects of Substrate Polarity and (In,Ga)N Buffer Layer on Polarity of GaN Films

	c(+)-ZnO substrate	c(–)-ZnO substrate
GaN/ZnO	c(–)-GaN	c(+)-GaN
GaN/InGaN/ZnO	c(+)-GaN	c(+)-GaN

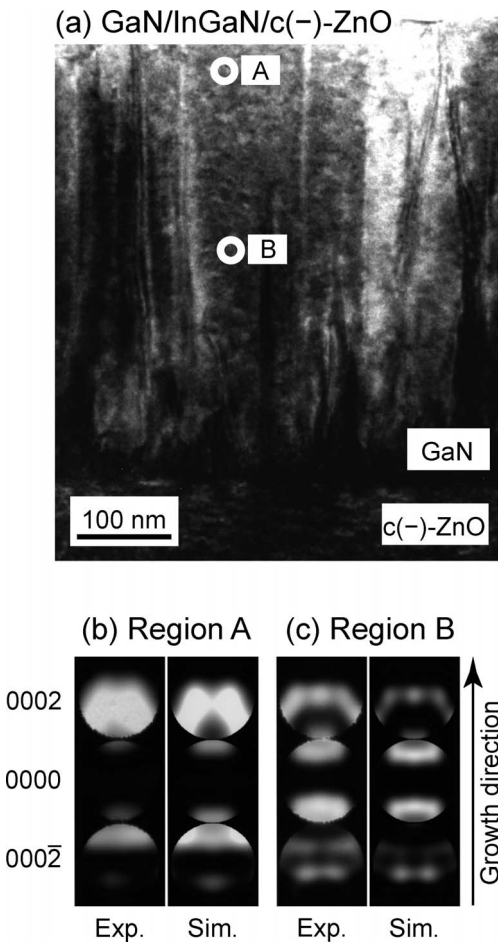

Fig. 6. (a) TEM image of GaN/InGaN/c(–)-ZnO structure and (b), (c) experimental and simulated CBED patterns of GaN film with (In,Ga)N buffer layer grown on c(–)-ZnO substrate; (b) near film surface (region A) and (c) center of film (region B). Simulated patterns in (b) and (c) correspond to 40- and 58-nm thickness of c(+)-GaN layer, respectively.

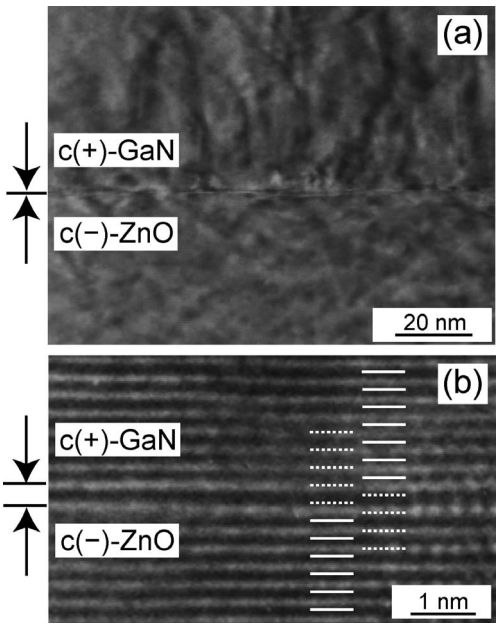

Fig. 7. TEM images of GaN film with (In,Ga)N buffer layer grown on c(–)-ZnO substrate: (a) interface region of heterostructure and (b) highly magnified image of interface.

was surprising to find that the interfaciel layer assumed to cause the polarity inversion was only a few atoms thick.

The detailed structure of the assumed inversion layer could not be determined because TEM imaging does not provide sufficient information for constructing a model of the atomic arrangement at the interface. However, a possible model for explaining polarity inversion at the GaN/ZnO interface is based on the assumption that there is a structural similarity between the GaN/ZnO interface, shown in Fig. 7, and the crystal structure of ZnO-based layered compounds. A structural element in a ZnO-based homologous structure,[41),42)] e.g., $In_2O_3(ZnO)_6$, is a candidate structure for explaining the polarity inversion. As shown in **Fig. 8(a)**, this homologous structure is composed of c(+)-ZnO layers, c(–)-ZnO layers, In_2O_3-like layers with octahedral coordination, and hexagonal boron-nitride (h-BN) like layers with planar coordination comprising In and O atoms, and these layers are alternatively stacked in the 0001 direction. In this crystal structure, the In_2O_3-like layer is sandwiched between Zn-terminated ZnO layers, and the h-BN-like layer is sandwiched between O-terminated ZnO layers. The polarity inversion at a GaN/ZnO interface only a few atoms thick can be explained on the basis of the analogy between polarity inversion at the GaN/ZnO interface and a similar elemental structure in the homologous structure. As shown in Fig. 8(b), the presence of the h-BN-like layer (Ga_2O_3 interfaciel layer) explains the c(+)-GaN/c(–)-ZnO structure, for which an h-BN-like layer can be assumed to be sandwiched between N-terminated (+)-GaN film and a O-terminated c(–)-ZnO substrate. In contrast, the presence of the In_2O_3-like layer (Ga_2O_3 interfaciel layer) at the GaN/ZnO interface explains the c(–)-GaN/c(+)-ZnO heterostructure, as shown in Fig. 8(c), for which an octahedral In_2O_3-like layer can be assumed to be sandwiched between Ga-terminated c(–)-GaN film and a Zn-terminated c(+)-ZnO substrate.

A GaN/ZnO heterostructure composed of a continuous wurtzite-lattice boundary without polarity inversion was achieved only when c(+)-ZnO substrates with an (In,Ga)N buffer layer were used. The existence of an interfaciel layer, even a few atoms thick, was not observed at the c(+)-GaN/InGaN/c(+)-ZnO interface. The reason for the absence of the polarity inversion layer for these growth conditions is not clear. It is known that the polarity of GaN films strongly depends on various growth processes, such as substrate nitridation, and the growth temperature.[33)] Understanding the polarity dependence of surface reactivity is probably the most important issue for understanding the formation of the inversion layer. Many studies have revealed a difference in chemical reactivity between c(+)- and c(–)-ZnO. For example, the chemical etching characteristics of ZnO[29)] and the reactivity of ZnO with nitrogen radicals[27)] depend on its crystalline polarity. Further study is required to clarify the formation of the polarity inversion layer and the mechanism of its formation in GaN/ZnO heterostructures.

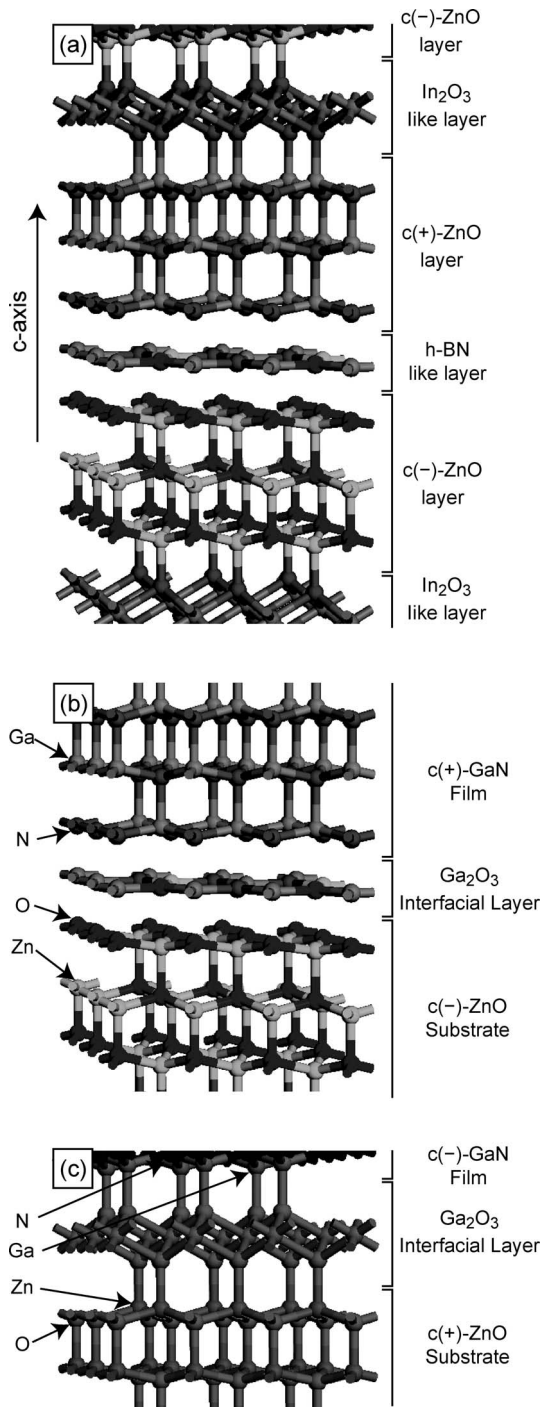

Fig. 8. Schematics of atomic arrangement of (a) $In_2O_3(ZnO)_6$ structure, (b) c(+)-GaN/c(–)-ZnO structure, and (c) c(–)-GaN/c(+)-ZnO structure.

4. Conclusion

GaN films were grown with and without lattice-matched (In,Ga)N buffer layers on the c(+) and c(–) faces of ZnO single-crystal substrates using molecular beam epitaxy. The structure and lattice relaxation mechanism of the films were strongly dependent on the polarity of the substrate and on the use of an (In,Ga)N buffer layer. GaN film grown on a c(+)-ZnO substrate had a rough surface and was composed of columnar grains, and that grown on a c(–)-ZnO substrate had a smooth surface with many threading dislocations parallel to the growth direction. In contrast, GaN films grown with (In,Ga)N buffer layers on both c(+)- and c(–)-ZnO substrates had the same structure as that grown directly on a c(–)-ZnO substrate, i.e., a relatively smooth surface with many threading dislocations. The (In,Ga)N buffer layer enables the use of high-temperature growth and causes gradual relaxation of the lattice mismatch, resulting in improved film crystallinity. The grown GaN films, except for that grown with an (In,Ga)N buffer layer on a c(+)-ZnO substrate, had polarity opposite that of the substrate. This was due to the polarity inversion layer formed at the ZnO surface. We found that a GaN/ZnO heterostructure composed of a continuous wurtzite-lattice boundary without polarity inversion can be achieved by using a buffer layer and a c(+)-ZnO substrate.

Acknowledgements The author wishes to express his gratitude to Dr. Hajime Haneda, Dr. Naoki Ohashi, and the members of the research group at the National Institute for Materials Science (NIMS) for their continuous support and suggestions. This study was primarily supported by the Projects for University Start-ups Creation promoted by the Ministry of Education, Culture, Sports, Science and Technology, Japan (FY2002–2003, no. 26) and partly supported by Special Coordination Funds for Promoting Science and Technology (Ceramics Integration Project) from the same ministry.

References

1) H. Amano, K. Sawaki, I. Akasaki and Y. Toyoda, *Appl. Phys. Lett.*, 48, 353–355 (1986).
2) H. Amano, M. Kito, K. Hiramatsu and I. Akasaki, *Jpn. J. Appl. Phys.*, 28, L2112–L2114 (1989).
3) S. Nakamura, *Jpn. J. Appl. Phys.*, 30, L1705–1707 (1991).
4) S. Nakamura, N. Iwasa, M. Senoh and T. Mukai, *Jpn. J. Appl. Phys.*, 31, 1258–1266 (1992).
5) J. Suda and H. Matsunami, *J. Cryst. Growth*, 237–239, 1114–1117 (2002).
6) C. Sasaoka, H. Sunakawa, A. Kimura, M. Nido, A. Usui and A. Sakai, *J. Cryst. Growth*, 189, 551–555 (1998).
7) K. Shimamura, E. G. Víllora, K. Domen, K. Yui, K. Aoki and N. Ichinose, *Jpn. J. Appl. Phys.*, 44, L7–L8 (2005).
8) D. G. Thomas, *J. Phys. Chem. Solid*, 15, 86–96 (1960).
9) Y. G. Wang, N. Ohashi, Y. Wada, I. Sakaguchi, T. Ohgaki and H. Haneda, *J. Appl. Phys.*, 100, 023524 (2006).
10) E. Ohshima, H. Ogino, I. Niikura, K. Maeda, M. Sato, M. Ito and T. Fukuda, *J. Cryst. Growth*, 260, 166–170 (2004).
11) A. Ohtomo, M. Kawasaki, T. Koida, K. Masubuchi, H. Koinuma, Y. Sakurai, Y. Yoshida, T. Yasuda and Y. Segawa, *Appl. Phys. Lett.*, 72, 2466–2468 (1998).
12) T. Ohgaki, Y. Kawamura, T. Kuroda, N. Ohashi, Y. Adachi, T. Tsurumi, F. Minami and H. Haneda, *Key Eng. Mater.*, 248, 91–94 (2003).
13) T. Tsurumi, S. Nishizawa, N. Ohashi and T. Ohgaki, *Jpn. J. Appl. Phys.*, 38, 3682–3688 (1999).
14) T. Nakayama and M. Murayama, *J. Cryst. Growth*, 214, 299–303 (2000).
15) C. Chen, M. Dutta and M. A. Stroscio, *J. Appl. Phys.*, 95, 2540–2546 (2004).
16) F. Hamdani, M. Yeadon, D. J. Smith, H. Tang, W. Kim, A. Salvador and A. E. Botchkarev, *J. Appl. Phys.*, 83, 983–990 (1998).
17) T. Ohgaki, S. Sugimura, H. Ryoken, N. Ohashi, I. Sakaguchi, T. Sekiguchi and H. Haneda, *Key Eng. Mater.*, 301, 79–82 (2005).
18) Y. I. Alivov, J. E. V. Nostrand, D. C. Look, M. V. Chukichev and B. M. Ataev, *Appl. Phys. Lett.*, 83, 2943–2945 (2003).
19) Q.-X. Yu, B. Xu, Q.-H. Wu, Y. Liao, G.-Z. Wang, R.-C. Fang, H.-Y. Lee and C.-T. Lee, *Appl. Phys. Lett.*, 83, 4713–4715 (2003).
20) A. Osinsky, J. W. Dong, M. Z. Kauser, B. Hertog, A. M. Dabiran, P. P. Chow, S. J. Pearton, O. Lopatiuk and L. Chernyak, *Appl. Phys. Lett.*, 85, 4272–4274 (2004).
21) S.-K. Hong, T. Hanada, H.-J. Ko, Y. Chen, T. Yao, D. Imai, K. Araki, M. Shinohara, K. Saitoh and M. Terauchi, *Phys. Rev. B*, 65, 115331 (2002).
22) F. Hamdani, A. E. Botchkarev, H. Tang, W. Kim and H. Morkoç, *Appl. Phys. Lett.*, 71, 3111–3113 (1997).
23) S. Chichibu, T. Azuhata, T. Sota and S. Nakamura, *Appl. Phys. Lett.*, 69, 4188–4190 (1996).
24) O. Ambacher, J. Smart, J. R. Shealy, N. G. Weimann, K. Chu, M. Murphy, W. J. Schaff, L. F. Eastman, R. Dimitrov, L. Wittmer, M. Stutzmann, W. Rieger and J. Hilsenbeck, *J. Appl. Phys.*, 85, 3222–3233 (1999).
25) N. Ohashi, K. Takahashi, S. Hishita, I. Sakaguchi, H. Funakubo and H. Haneda, *J. Electrochem. Soc.*, 154, D82–D87 (2007).
26) N. Ohashi, T. Ohgaki, S. Sugimura, K. Maeda, I. Sakaguchi, H. Ryoken, I. Niikura, M. Sato and H. Haneda, *Mat. Res. Soc. Symp. Proc.*, 799, 255–260 (2004).
27) H. Maki, I. Sakaguchi, N. Ohashi, S. Sekiguchi, H. Haneda, J. Tanaka and N. Ichinose, *Jpn. J. Appl. Phys.*, 42, 75–77 (2003).
28) A. Tsukazaki, A. Ohtomo, T. Kita, Y. Ohno, H. Ohno and M. Kawasaki, *Science*, 315, 1388–1391 (2007).
29) H. Iwanaga and N. Shibata, *Jpn. J. Appl. Phys.*, 6, 415 (1967).
30) M. Katayama, E. Nomura, N. Kanekama, H. Soejima and M. Aono, *Nucl. Instr. and Meth. B*, 33, 857–861 (1988).
31) Z. Liliental-Weber, J. Washburn, K. Pakula and J. Baranowski, *Microsc. Microanal.*, 3, 436–442 (1997).
32) T. Ohgaki, N. Ohashi, H. Haneda and A. Yasumori, *J. Cryst. Growth*, 292, 33–39 (2006).
33) M. Sumiya, M. Tanaka, K. Ohtsuka, S. Fuke, T. Ohnishi, I. Ohkubo, M. Yoshimoto, H. Koinuma and M. Kawasaki, *Appl. Phys. Lett.*, 75, 674–676 (1999).
34) S. Sonoda, S. Shimizu, Y. Suzuki, K. Balakrishnan, J. Shirakashi, H. Okumura, T. Nishihara and M. Shinohara, *Jpn. J. Appl. Phys.*, 38, L1219–L1221 (1999).
35) T. Ohnishi, A. Ohtomo, M. Kawasaki, K. Takahashi, M. Yoshimoto and H. Koinuma, *Appl. Phys. Lett.,* 72, 824–826 (1998).
36) M. Stutzmann, O. Ambacher, M. Eickhoff, U. Karrer, A. Lima Pimenta, R. Neuberger, J. Schalwig, R. Dimitrov, P. J. Schuck and R. D. Grober, *Phys. Stat. Sol. (b)*, 228, 505–512 (2001).
37) D. Huang, P. Visconti, K. M. Jones, M. A. Reshchikov, F. Yun, A. A. Baski, T. King and H. Morkoç, *Appl. Phys. Lett.*, 78, 4145–4147 (2001).
38) H. Matsui, H. Saeki, T. Kawai, A. Sasaki, M. Yoshimoto, M. Tsubaki and H. Tabata, *J. Vac. Sci. Technol. B*, 25, 2454–2461 (2004).
39) T. Ohgaki, S. Sugimura, N. Ohashi, I. Sakaguchi, T. Sekiguchi and H. Haneda, *J. Cryst. Growth*, 275, e1143–e1148 (2005).
40) T. Ohgaki, N. Ohashi, T. Ohnishi, H. Haneda, M. Lippmaa and A. Yasumori, *J. Ceram. Soc. Japan*, 115, 414–418 (2008).
41) N. Kimizuka, M. Isobe and M. Nakamura, *J. Solid State Chem.*, 116, 170–178 (1995).
42) Y. Takeda, K. Nomura, H. Ohta, H. Yanagi, T. Kamiya, M. Hirano and H. Hosono, *Thin Solid Films*, 486, 28–32 (2005).

Takeshi Ohgaki is a researcher at the National Institute for Materials Science (NIMS). He received B. Eng., M. Eng. and Dr. Eng. degrees from the Tokyo Institute of Technology in 1997, 1999, and 2002. He worked at NIMS as a post-doctoral researcher from 2002 to 2005 and at the Tokyo University of Science as a research associate from 2005 to 2007. In 2007, he joined the Sensor Materials Center at NIMS. His research interests are crystal growth and interface control of oxide and nitride materials for electric and optical applications.